



Identification of Subsurface Structures Using Topex Altimetry Satellite Gravity Data: Implications for Preliminary Surveys of Geothermal Existence

Dwi Anggraeni*

Department of Physics,
Institut Teknologi Sumatera,
INDONESIA

Rahmat Nawi Siregar

¹Department of Physics,
Institut Teknologi Sumatera,
INDONESIA

²Department of Physics,
Universitas Gadjah Mada,
INDONESIA

Sismanto

Department of Physics,
Universitas Gadjah Mada,
INDONESIA

*Correspondence: E-mail: anggraenidwi993@gmail.com

Article Info

Article history:

Received: May 15, 2023

Revised: June 30, 2023

Accepted: August 16, 2023



Copyright : © 2022 Foundae (Foundation of Advanced Education). Submitted for possible open access publication under the terms and conditions of the Creative Commons Attribution - ShareAlike 4.0 International License (CC BY SA) license (<https://creativecommons.org/licenses/by-sa/4.0/>).

Abstract

Bangka Island is on the Sunda Shelf (Eurasian tectonic plate) and the outer part of the Sumatra basin. Plate tectonic activity results in fault structures and forms the stratigraphy of rock formations such as Alluvium, Ranggam, Klabat Granite, Tanjung Genting, and the Pemali Complex. The fault structure was identified as a control structure for the radiogenic geothermal system. Radiogenic geothermal heat originates from the decay of radioactive elements in granite rocks (Klabat Granite formation) on Bangka Island. The purpose of this research is as a preliminary survey of the presence of Slag and Cracker geothermal energy on Bangka Island using the gravity method. The research data used is secondary data obtained from the Topex satellite (Topography Experiment). The results of the modeling show that many fault structures in the study area are found around the Slag and Cracking geothermal manifestations. The fault structure is also accompanied by a breakthrough by the lower layer of rock into the rock above it. So that the fault structure can control the Slag and Crack radiogenic geothermal system.

Keywords: density; gravity; fault; topex; geothermal existence

To cite this article: Anggraeni, D., Siregar, R, N, and Sismanto. (2023). Identification of Subsurface Structures Using Topex Altimetry Satellite Gravity Data: Implications for Preliminary Surveys of Geothermal Existence. *International Journal of Hydrological and Environmental for Sustainability*, 2(2), 88-96. <https://doi.org/10.58524/ijhes.v2i2.261>

INTRODUCTION

The Eurasian Plate, as a plate that is still active, has an influence on the tectonic setting of Bangka Island, namely the formation of structures on Bangka Island, Indonesia and has an influence on the formation of basin areas, either lowering or lifting the base of the basin in the original rock area (Lange et al., 2018; Liu et al., 2021; McCaffrey, 2009). The effects that occur due to the subsidence or uplift of the basin floor are changes in the depositional environment (sedimentation process) (Hanus et al., 1996; Malod et al., 1995).

The Sunda Shelf connects lands such as the Kalimantan region to the west through the Natuna region to the Malay Peninsula region, in the southern part includes the Java Sea region, in the north-western part of Java and the most north-eastern part of Sumatra. Bangka Island and the small islands around Sumatra Island are included in the Sunda Shelf (Hanus et al., 1996; Lange et al., 2018). The Sunda Shelf is a landform on the Eurasian continental plate which was formed due to the influence of climate change during the Pleistocene-Holocene period and the influence of changes in sea level.

When there is a shift and collision between tectonic plates such as the India-Australia, Pacific, Philippine, Eurasia Plates, and changes in sea level cause sea levels to fall. Then the Sunda Shelf was formed as a very wide swamp land on the Eurasian continental plate (Hochstein & Sudarman, 1993; Utama et al., 2021).

Bangka Island is part of the Sunda Shelf, as well as the outer part of the Sumatran back arc basin. The basin will become an economical reservoir/trap for hydrocarbons as a place for the sedimentation process to take place. One of the sedimentation processes that occurs is producing granite rocks. The granite on Bangka Island is experiencing changes caused by the presence of faults or joints, so that the granite can break through the bedrock on Bangka Island (Siregar & Kurniawan, 2018).

Granite rocks in Bangka were formed from the freezing of magma during the Triassic-Jurassic period, which is included in the Klabat Granite group. Granite and sandstone rocks that have been intensively deformed are thought to have fractured joints so that they become good geothermal reservoirs. Granite rocks in the Bangka area contain the main concentrations of Cerium (Ce), Lanthanum (La), Yttrium (Y), and Thorium (Th) which form the mineral monazite (ADB & Bank, 2015; Deon et al., 2015; Giggenbach, 1991; Meijaard et al., 2019). Research related to the study of monazite and zircon deposits in the Cerucuk Belitung area. The presence of radioactive minerals was detected at quite high radioactivity values of 40-400 c/s, the radioactivity of heavy minerals was 250-1,000 c/s, the Th content (100-6,545 ppm) was higher than U (15-639.4 ppm) in monazite. Monazite has resistant properties with a density of 4.4-5.5 gr/cm³, monazite will be transported with other minerals and sedimented in the new environment (Darma et al., 2010; Millot et al., 2007; Nafian et al., 2022; Winters & Cawvey, 2015).

The geothermal control structure on Bangka Island was formed due to the tectonic activity of the Eurasian Plate. Tectonic activity causes forces to deform rocks and forms structures in the form of folds, faults, joints and fractures. The geothermal control structure is an access that connects the heat source to the manifestation of geothermal heat on the surface. Thus, a non-volcanic geothermal system in the research area can be formed (Hochstein & Sudarman, 1993; Kruger et al., 1977; Millot et al., 2012; Utama et al., 2021).

Examples of non-volcanic geothermal systems in the Bangka Island region are the Terak and Kerak geothermal systems. The Slag and Cracking geothermal heat gives rise to manifestations in the form of hot water (61.8°C) thought to be caused by the presence of hot meteoric water that has accumulated below the surface. Research on non-volcanic geothermal systems, especially radiogenic geothermal systems such as Slag and Kerak, is currently being studied by many researchers. One of the studies in the Keretak geothermal area was by previous research with the aim of obtaining information on the subsurface structure, distribution of granite and the volume of granite in the area of radiogenic geothermal manifestation. The research results obtained were in the form of subsurface structures of sedimentation layers, granite intrusions (depth 0-200 m with a granite volume of around 3,937,934.02 m³) and river sediments (Darmawan et al., 2015; Matsubaya et al., 1973; Takahashi et al., 2000; Timperley & Vigor-Brown, 2010; W.F. Giggenbach, 1992).

In 2017, the Ministry of Energy and Mineral Resources described the potential of the Terak geothermal area as a non-volcanic geothermal system (Utama et al., 2021). The rocks that make up the area are surface deposits, metamorphic rocks (Permo-Carboniferous), old plutonic igneous rocks in the form of granite (Triassic) and alluvium deposits. The structures that dominate the area are normal and strike-slip faults in a northwest-southeast direction and strike-slip faults in a northeast-southwest direction. This occurs because of the uniqueness of the radiogenic geothermal source which originates from radioactive decay in the constituent rocks in the Terak and Krek areas (Hanuš et al., 1996; Hochstein & Sudarman, 1993; Lange et al., 2018; Liu et al., 2021; McCaffrey, 2009). In addition, the uniqueness of the radiogenic geothermal system in the study area does not cause any alteration rocks to form. This research is important to carry out because there is not much research that discusses geothermal slag and cracks, especially using the gravity method.

METHOD

The time of the research was carried out from December 2021 to May 2022. The research location in this final project was Central Bangka Regency, the Terak and Keretak geothermal location. The research area is in a geographical position with coordinates $2^{\circ}0'48.78''$ - $2^{\circ}30'27.01''$ LS and $105^{\circ}42'10.58''$ - $106^{\circ}27'3.66''$ BT. Data collection was carried out on March 20 2022 at 08.00 WIB. Data collection was not carried out directly in the research area, but used secondary data from Topex. Then the research data processing was carried out at the Earth Physics Laboratory, Physics Study Program, Science Department, Sumatra Institute of Technology, Lampung, Indonesia.

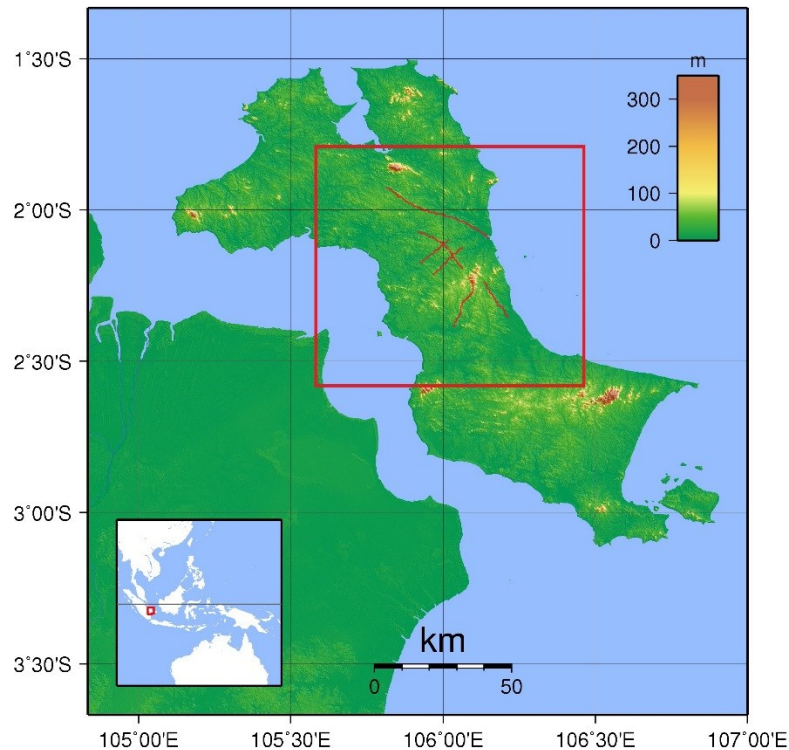


Figure 1. Research location map ; the red line is the research area (modify from https://id.wikipedia.org/wiki/Pulau_Bangka)

Data Type

The research data in this final project is in the form of secondary data taken from Topex satellite imagery. The data required in processing the gravity method is elevation data from measurement points and Free Air Anomaly value data. Data collection can be done via the website <http://topex.ucsd.edu/>.

Data analysis

This research uses secondary data using Topex satellite image data. The research process was carried out using customized software to be able to process gravity data. Microsoft Excel software was used to combine topographic and gravitational data and calculate simple Bouguer correction values. Oasis Montaj software is used to carry out terrain correction, create anomaly maps, anomaly separation, spectrum analysis and two-dimensional modeling. Surfer16 software was used for data gridding, the latter software Grablox 1.6 e was used for three-dimensional modeling and opened using Bloxer 1.6 e for advanced interpretation with Complete Bouguer Anomaly data.

RESULTS AND DISCUSSION

Bangka Island is in the Sunda Shelf area (Sundaland Craton of the Eurasian Plate). Tectonic activity by the Eurasian Plate causes forces that can deform rocks on Bangka Island. The deformation of the rock forms structures in the form of joints, folds, faults and straightness. Joint and fault structures

are related to folding. Folds in the rock produce rock formations, namely, the Ranggalang Formation and the Tanjung Genting Formation. This rock formation is thought to be the result of deformation of rocks older than the Mesozoic era. Based on geological data obtained from the Indonesian SHP map, using QGIS tools a regional geological map and stratigraphy of the research area was created. Stratigraphy of rock sedimentation results on Bangka Island produces the formation of the Sandstone Unit (TRp), Permian Granite Unit (TJg), surface deposits in the form of Swamp and Beach Deposits (Qs) and Alluvium (Qa).

Bouguer Anomaly Analysis

The results of the Bouguer anomaly analysis were obtained after calculating gravity data. The complete Bouguer anomaly map is used to display the distribution pattern of subsurface rock density values. **Figure 2** is the result of a complete Bouguer anomaly map of the area around the Terak and Cracking geothermal area in UTM coordinates, with a range of anomaly values shown on a bar scale ranging from 23.7 to 40.9 mGal. The anomaly value from the complete Bouguer anomaly map is comparable to the rock density value in the study area.

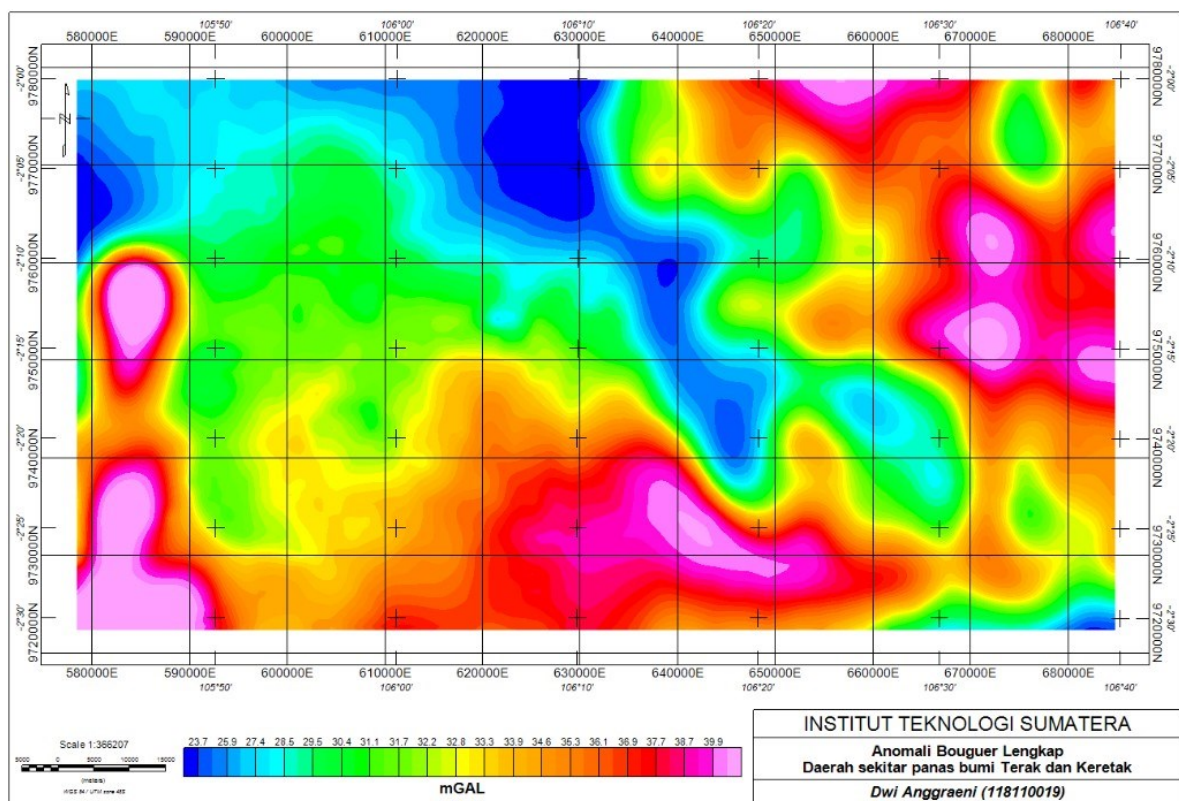


Figure 2. Bouguer anomaly map of the area around the Terak and Kerak geothermal areas

Low anomaly values indicate the presence of low rock density, such as in the blue to light blue areas which are identified as the dominance of the Alluvium formation. It is estimated that the alluvium formation has a density of between 1.63 gr/cm^3 to 2.0 gr/cm^3 , because it consists of swamp deposits (sand and mud), gravel, gravel and clay. Then high anomaly values with red to pink colors indicate the presence of high rock density, such as granite rock intrusions found on Bangka Island with density values of $2.5\text{--}2.81 \text{ gr/cm}^3$. The granite on Bangka Island is estimated to be Early Triassic in age and was deposited in shallow seas (Hanus̄ et al., 1996; Hochstein & Sudarman, 1993).

Spectrum Analysis

Spectrum analysis is carried out by converting spatial data into spectral data in the wavelength domain, using the Fourier transformation. Fourier transformation produces estimated data on the depth of the anomaly source, wave number and logarithm of amplitude (Li et al., 2016). Spectrum

analysis was carried out to determine each depth value of the residual, regional and noise areas in the research area.

In order to obtain an estimate of the depth of these three areas, a curve was created between the wave number and the logarithm of the amplitude. Then three gradient values are created on the curve which show three regional areas, residual and noise with different values. After that, the coefficient of determination is also displayed which is used as the boundary of the three regional areas, residual and noise. The relationship curve between the wave number values and the logarithm of the amplitude is shown in **Figure 3**.

Figure 3 shows that there is an area bounded by a black line. If you look at the Fourier transformation data, you will see that the intersection of the black line and the wave number axis is 0.03. This value is the boundary value between the regional area and the residual. Then, to find out the wavenumber value that limits the residual and noise areas, the blue line intersects the wavenumber axis at a value of 0.17. The waveform value as the limit will be used to estimate the depth value of the anomaly source by drawing a vertical line on the spectrum analysis curve and depth estimation curve as shown in **Figure 4**.

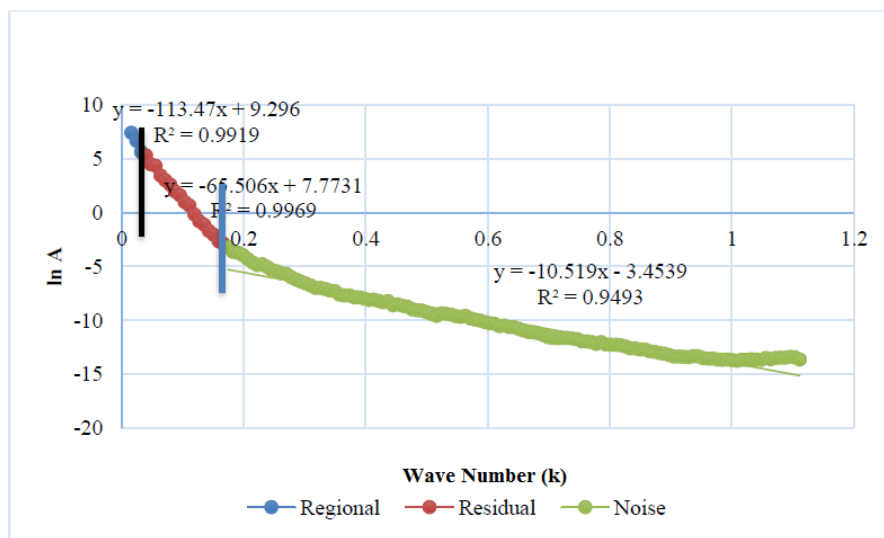


Figure 3. Spectrum analysis curve

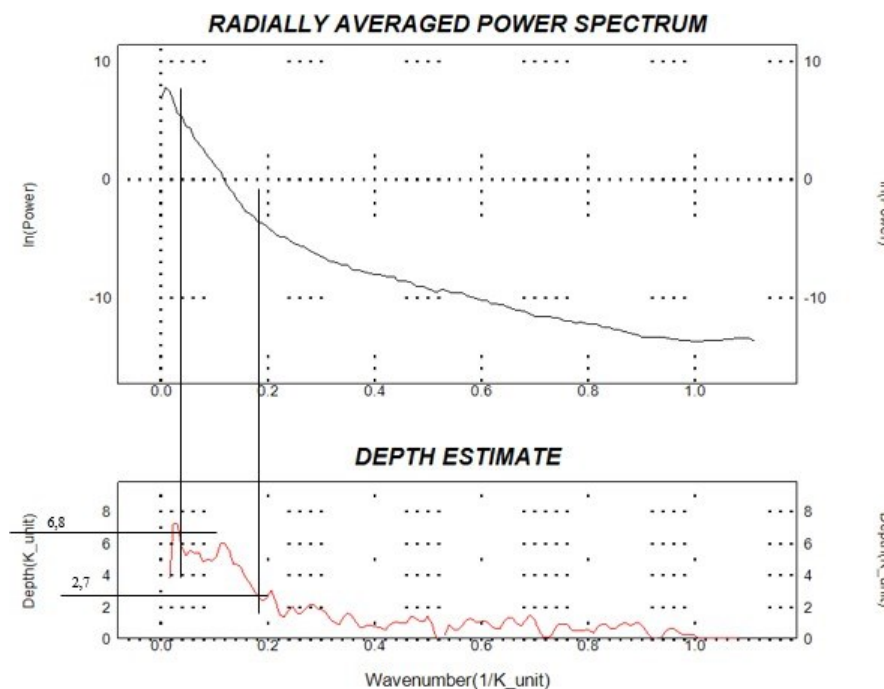


Figure 4. Spectrum analysis curve and depth estimation

Based on **Figure 4** and adjusted to data from Fourier transformation values, the value with a wave number of 0.03 is at a depth of 6.8 km, which is assumed to be the regional and residual area boundary. Then at a wave number of 0.17 the depth is estimated to be 2.7 km, which is the boundary between the residual and noise areas.

Separation of Residual and Regional Anomalies

Separation of residual, regional and noise anomalies is carried out through a complete Bouguer anomaly map. A complete Bouguer anomaly map needs to be separated from each of its components, so that the source of the shallow anomaly as a residual anomaly and the source of the deep anomaly as a regional anomaly can be identified. One way to separate residual and regional anomalies is by using the bandpass filter and lowpass filter methods. Bandpass filters are used to separate residual anomalies, by removing wave numbers with a certain range of values so that they can display a residual anomaly map. Then using a lowpass filter, regional anomaly separation is carried out by removing high wave numbers to display low wave numbers, namely the regional anomaly map. The residual anomaly map is shown in **Figure 5** and the regional anomaly map is shown in **Figure 6**.

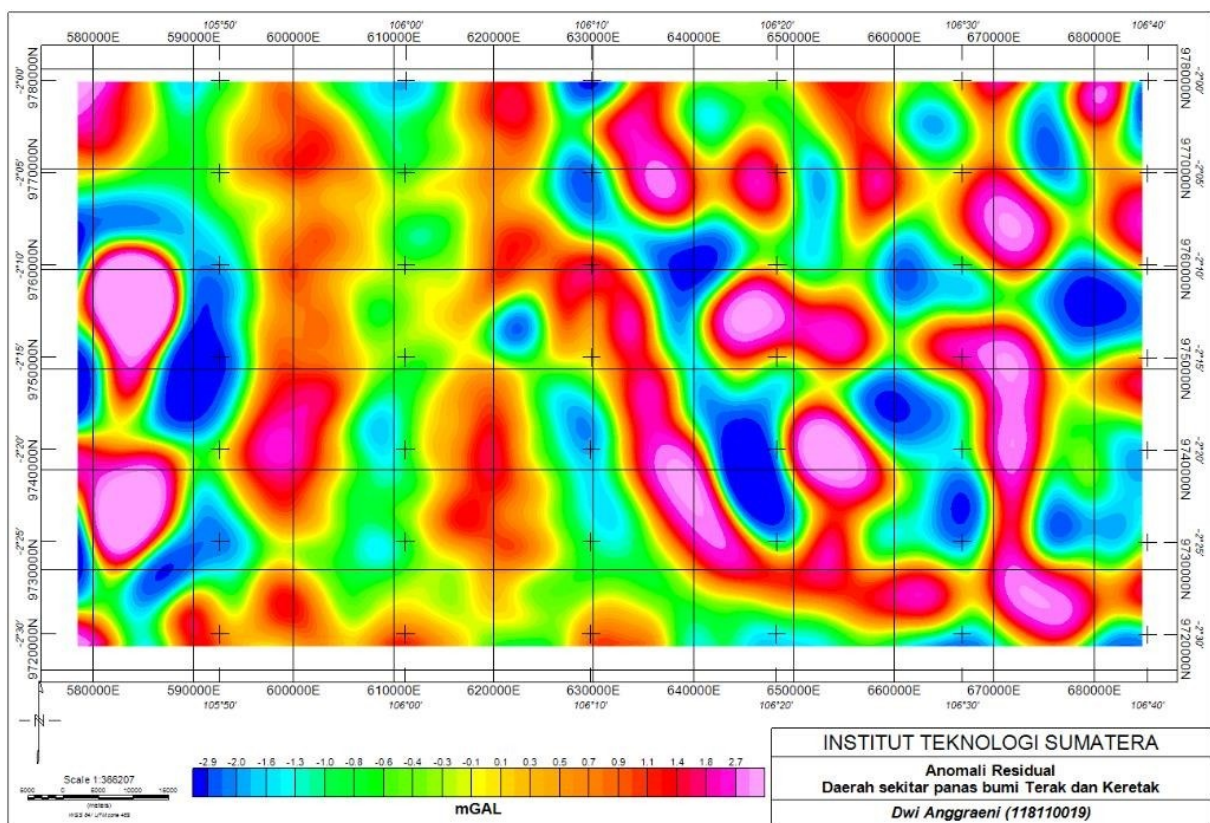


Figure 5. Residual anomaly map

Based on the residual anomaly map, it can be seen that the anomaly values can be divided into three patterns, namely low anomaly, medium anomaly and high anomaly. Low anomaly values range from -2.9 mGal to -1.1 mGal, with a blue to light blue color orientation. The moderate anomaly section has values in the range of -1.0 mGal to 0.9 mGal, marked in green to orange. High anomaly sections are shown in red to pink, with values ranging from 1.0 mGal to 3.4 mGal.

Low anomalies on the residual anomaly map are identified as Alluvium formations, swamp deposits and quartz sand. Where the rocks that make up the formation have low rock density values such as sand, clay, gravel, gravel and mud. Meanwhile, the high anomalies contained in the residual anomaly map are identified as granite rock breaking through the

rocks above it such as sandstone, malihan sandstone, clayey sandstone and claystone with limestone lenses which form the Tanjung Genting formation. The Tanjung Genting Formation is of Triassic age which has experienced folding, spreading and faulting, so that it can be intruded by granite.

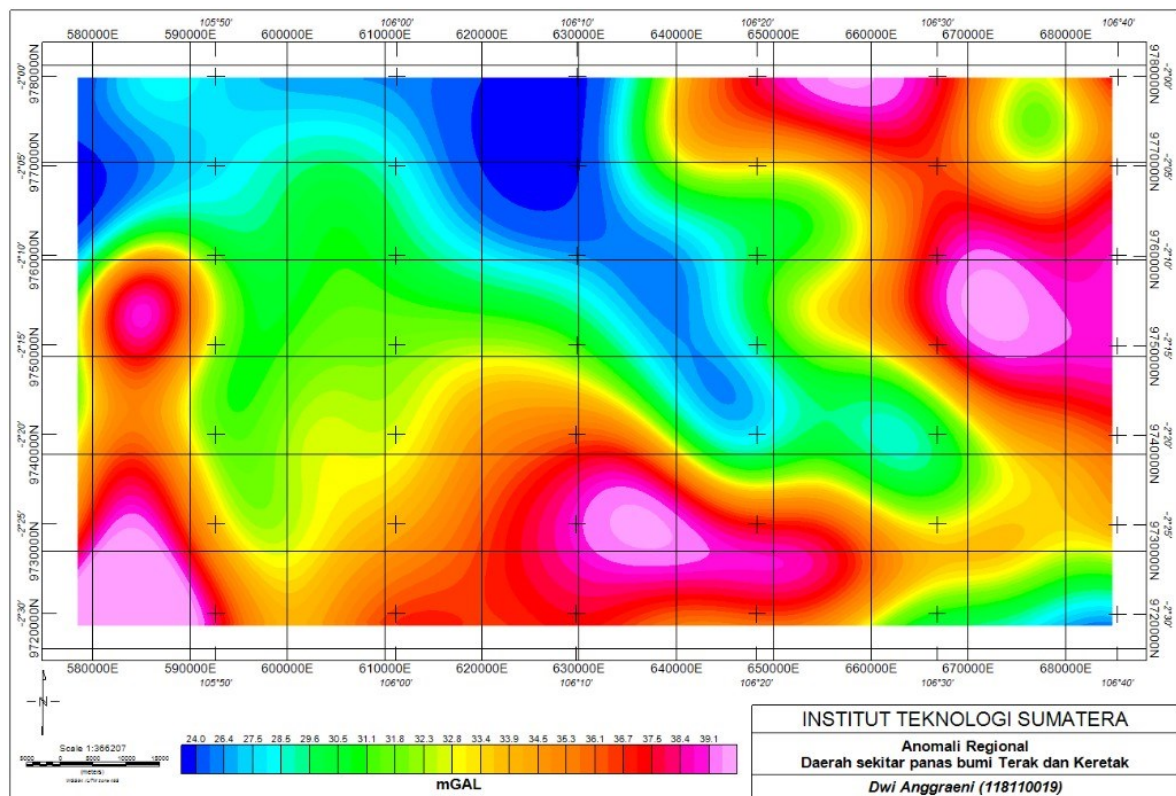


Figure 6. Regional anomaly map

The regional anomaly map is divided into two parts of anomaly values, namely low anomalies and high anomalies. The northeastern to northern parts of the study area are areas with low anomalies with blue to light blue colors. The range of low anomaly values is 24.0 mGal to 29.1 mGal. Meanwhile, high anomalies are in the east, southeast, south, west and northwest positions in the study area, with anomaly values of 34.9 mGal to 39.8 mGal. Colors that indicate high anomalies are represented by orange to pink.

The research area consists of the Klabat Granite formation, Tanjung Genting and the Pemali Complex at deeper depths. The high anomalous value was identified as granite which is part of the Klabat Granite formation. There are more patterns of high anomaly values on regional anomaly maps than patterns of low anomaly values, this is because the Klabat Granite formation dominates the study area at deeper depths. Meanwhile, the pattern of low anomaly values found on the regional anomaly map is identified as sandstone that forms the Tanjung Genting formation. Where the Tanjung Genting formation consists of rock material that is less conductive over granite.

CONCLUSION

As a result of complete Bouguer anomaly modeling, the subsurface layers of the area around the Terak and Kerak geothermal areas consist of several rock formations and fault structures. Rock formations from the first layer are Holocene alluvium formation, Triassic Tanjung Genting, Triassic-Jurassic Klabat granite, Pemali formation as bedrock. There are many fault structures in the research area around the Slag and Cracking geothermal manifestations. The fault structure is also accompanied by a breakthrough by the lower layer of rock into the rock above it.

CONFLICTS OF INTEREST

The authors declare no conflict of interest concerning the publication of this article. The authors also confirm that the data and the article are free of plagiarism.

REFERENCES

- ADB, & Bank, W. (2015). *Unlocking Indonesia's Geothermal Potential*. <https://creativecommons.org/licenses/by/3.0/igo/>. By
- Darma, S., Harsoprayitno, S., Setiawan, B., Hadyanto, Sukhyar, R., Soedibjo, A. W., Ganefianto, N., & Stimac, J. (2010). Geothermal Energy Update: Geothermal Energy Development and Utilization in Indonesia. *Proceedings of World Geothermal Congress 2010, April*, 1–13.
- Darmawan, I. G. B., Setijadji, L. D., & Wintolo, D. (2015). Geology and Geothermal System in Rajabasa Volcano South Lampung Regenc , Indonesia (Approach to Field Observations , Water Geochemistry and Magnetic Method). *Proceedings World Geothermal Congress 2015, April*, 12.
- Deon, F., Förster, H. J., Brehme, M., Wiegand, B., Scheytt, T., Moeck, I., Jaya, M. S., & Putriatni, D. J. (2015). Geochemical/hydrochemical evaluation of the geothermal potential of the Lamongan volcanic field (Eastern Java, Indonesia). *Geothermal Energy*, 3(1), 1–21. <https://doi.org/10.1186/s40517-015-0040-6>
- Giggenbach, W. F. (1991). Chemical Techniques in Geothermal Exploration. In *Chemistry Division* (pp. 119–144).
- Hanuš, V., Špičák, A., & Vaněk, J. (1996). Sumatran segment of the Indonesian subduction zone: Morphology of the Wadati-Benioff zone and seismotectonic pattern of the continental wedge. *Journal of Southeast Asian Earth Sciences*, 13(1), 39–60. [https://doi.org/10.1016/0743-9547\(96\)00004-9](https://doi.org/10.1016/0743-9547(96)00004-9)
- Hochstein, M. P., & Sudarman, S. (1993). Geothermal resources of Sumatra. *Geothermics*, 22(3), 181–200. [https://doi.org/10.1016/0375-6505\(93\)90042-L](https://doi.org/10.1016/0375-6505(93)90042-L)
- Kruger, P., Stoker, A., & Umaña, A. (1977). Radon in geothermal reservoir engineering. *Geothermics*, 5(1–4), 13–19. [https://doi.org/10.1016/0375-6505\(77\)90004-9](https://doi.org/10.1016/0375-6505(77)90004-9)
- Lange, D., Tilmann, F., Henstock, T., Rietbrock, A., Natawidjaja, D., & Kopp, H. (2018). Structure of the central Sumatran subduction zone revealed by local earthquake travel-time tomography using an amphibious network. *Solid Earth*, 9(4), 1035–1049. <https://doi.org/10.5194/se-9-1035-2018>
- Li, Y., Qiu, W., Qin, F., Fang, H., Hadjiev, V. G., Litvinov, D., & Bao, J. (2016). Identification of cobalt oxides with Raman scattering and Fourier transform infrared spectroscopy. *The Journal of Physical Chemistry C*, 120(8), 4511–4516. <https://doi.org/https://doi.org/10.1021/acs.jpcc.5b11185>
- Liu, S., Suardi, I., Xu, X., Yang, S., & Tong, P. (2021). The Geometry of the Subducted Slab Beneath Sumatra Revealed by Regional and Teleseismic Traveltime Tomography. *Journal of Geophysical Research: Solid Earth*, 126(1), 1–29. <https://doi.org/10.1029/2020JB020169>
- Malod, J. A., Karta, K., Beslier, M. O., & Zen, M. T. (1995). From normal to oblique subduction: Tectonic relationships between Java and Sumatra. *Journal of Southeast Asian Earth Sciences*, 12(1–2), 85–93. [https://doi.org/10.1016/0743-9547\(95\)00023-2](https://doi.org/10.1016/0743-9547(95)00023-2)
- Matsubaya, O., Sakai, H., Kusachi, I., & Satake, H. (1973). Hydrogen and oxygen isotopic ratios and major element chemistry of Japanese thermal water systems. *Geochemical Journal*, 7(3), 123–151. <https://doi.org/10.2343/geochemj.7.123>
- McCaffrey, R. (2009). The tectonic framework of the sumatran subduction zone. *Annual Review of Earth and Planetary Sciences*, 37, 345–366. <https://doi.org/10.1146/annurev.earth.031208.100212>

- Meijaard, E., Dennis, R. A., Saputra, B. K., Draugelis, G. J., Qadir, M. C. A., & Garnier, S. (2019). Rapid Environmental and Social Assessment of Geothermal Power Development in Conservation Forest of Indonesia. *Proceedings World Geothermal Congress 2020 Reykjavik, Iceland, April 26 – May 2, 2020, August*, 1–12.
- Millot, R., Hegan, A., & Negrel, P. (2012). Geothermal waters from the Taupo Volcanic Zone, New Zealand: Li, B, and Sr isotopes characterization. *Applied Geochemistry*, 27, 677–688. <https://doi.org/doi:10.1016/j.apgeochem.2011.12.015>
- Millot, R., Negrel, P., & E Petelet, giraud. (2007). Multi-isotopic (Li, B, Sr, Nd) approach for geothermal reservoir characterization in the Limagne Basin (Massif Central, France). *Applied Geochemistry*, 22(11), 2307–2325. <https://doi.org/https://doi.org/10.1016/j.apgeochem.2007.04.022>
- Nafian, M., Gunawan, B., Permana, N. R., & Umam, R. (2022). Identification of the Subsurface Structure of Geothermal Working Area of the Hamiding Mountain , North Maluku through Land Surface Temperature (LST) Data and Forward Modeling with the Gravity Method. *J. Nat. Scien. & Math. Res*, 8(1), 10–19.
- Siregar, R. N., & Kurniawan, W. B. (2018). 2D Interpretation of Subsurface Hot Spring Geothermal Structure in Nyelanding Village Through Schlumberger Geoelectricity Configuration Method. *Jurnal Ilmiah Pendidikan Fisika Al-Biruni*, 7(1), 81. <https://doi.org/10.24042/jipfalbiruni.v7i1.2324>
- Takahashi, M., Urai, M., Yasukawa, K., Muraoka, H., Matsuda, K., & Akasako, H. (2000). Geochemistry of Hot Spring Waters At Bajawa Area , Central Flores , Nusa Tenggara Timur , Indonesia. *Western Pacific Earth Sciences*, 1807–1812.
- Timperley, M. H., & Vigor-Brown, R. J. (2010). Water chemistry of lakes in the taupo volcanic zone, new zealand. *New Zealand Journal of Marine and Freshwater Research*, 20(2), 173–183. <https://doi.org/10.1080/00288330.1986.9516141>
- Utama, H. W., Mulyasari, R., & Said, Y. M. (2021). Geothermal Potential on Sumatra Fault System To Sustainable Geotourism in West Sumatra. *Jurnal Geofisika Eksplorasi*, 7(2), 126–137. <https://doi.org/10.23960/jge.v7i2.128>
- W.F. Giggenbach. (1992). Isotopic shifts in waters from geothermal and volcanicsystems along convergent plate boundaries and their origin. *Earth and Planetary Science Letters*, 113(4), 495–510.
- Winters, M. S., & Cawvey, M. (2015). Governance obstacles to geothermal energy development in Indonesia. *Journal of Current Southeast Asian Affairs*, 34(1), 27–56. <https://doi.org/10.1177/186810341503400102>